IKP-MS-93/0301

Effective source sizes of low rapidity soft particle emission

WA80 Collaboration

INSTITUT FÜR KERNPHYSIK
UNIVERSITÄT MÜNSTER

preprint IKP-MS-93/0301

Effective source sizes of low rapidity soft particle emission

T. Peitzmann
for the
WA80 Collaboration

Talk presented at
International Conference on Physics and Astrophysics
of the Quark-Gluon Plasma
Calcutta, January 1993

Effective source sizes of low rapidity soft particle emission

WA80 Collaboration

T. Peitzmann[4], R. Albrecht[1], T.C. Awes[5], P. Beckmann[4,a], F. Berger[4,b], M. Bloomer[2], C. Blume[4], D. Bock[4], G. Claesson[3], G. Clewing[4], L. Dragon[4,c], A. Eklund[3], R.L. Ferguson[5], A. Franz[5,a], S. Garpman[3], R. Glasow[4], H.Å. Gustafsson[3], H.H. Gutbrod[1], G. Hölker[4], J. Idh[3], P. Jacobs[2], K.H. Kampert[4], B.W. Kolb[1], H. Löhner[6], I. Lund[6], F.E. Obenshain[5], A. Oskarsson[3], I. Otterlund[3], F. Plasil[5], A.M. Poskanzer[2], M. Purschke[4], B. Roters[4], S. Saini[5], R. Santo[4], H.R. Schmidt[1], S.P. Sørensen[5,7], K. Steffens[4], P. Steinhaeuser[4], E. Stenlund[3], D. Stüken[4] and G.R. Young[5]

1. Gesellschaft für Schwerionenforschung, D-6100 Darmstadt, Fed. Rep. of Germany
2. *Lawrence Berkeley Laboratory, Berkeley, California 94720, USA*
3. *University of Lund, S-22362 Lund, Sweden*
4. *University of Münster, D-4400 Münster, Fed. Rep. of Germany*
5. *Oak Ridge National Laboratory, Oak Ridge, Tennessee 37831, USA*
6. *KVI, University of Groningen, NL-9747 AA Groningen, Netherlands*
7. *University of Tennessee, Knoxville, Tennessee 37996, USA*

a. *now at: CERN, CH-1211 Geneva 23, Switzerland*
b. *now at: Siemens AG, D-8000 Munich, Fed. Rep. of Germany*
c. *now at: Mercedes-Benz, D-7000 Stuttgart, Fed. Rep. of Germany*

Abstract

Correlations of positive pions and protons measured with the Plastic Ball detector in ultrarelativistic nucleus-nucleus collisions are studied. Source parameters are extracted for various projectile-target combinations. While the proton source can be explained by geometry, the pion source shows more subtle effects, which may be related to a very large source component.

1 Introduction

Correlations of identical particles allow a study of the emitting source in high energy collisions. Two-proton correlations exhibit a characteristic peak structure related to the ^{2}He-resonance. Two-pion correlations show an enhancement in the production for small relative momenta – known as Bose-Einstein correlations, the Hanbury-Brown - Twiss effect (HBT) [1] or the Goldhaber - Goldhaber - Lee - Pais effect (GGLP) [2]. Both these effects yield information on the space-time properties of the particle production.

In two-proton correlations one has to deal with effects of both strong and Coulomb final state interaction and Fermi-Dirac statistics. The most useful feature of these is the resonant behavior of the attractive mutual strong interaction. The more proton pairs are produced within the range of the interaction, the stronger is the resonance. As a consequence, the strength of the two-proton correlation increases for decreasing source size. For a realistic theoretical correlation function

	protons	pions
identification	$\Delta E - E$	$\Delta E - E$ & π^+-decay
resolution σ_Q	$\approx$ 30 MeV	$\approx$ 10 MeV
rapidity y_{lab}	-0.6 – 0.6	-1 – 1
transv. mom. p_T	100 MeV/c – 700 MeV/c	40 MeV/c – 200 MeV/c
misidentification	5% – 13%	< 5%

Table 1: Particle identification and acceptance of the Plastic Ball detector

one has to calculate the relative wave function including all the above-mentioned effects [3]. In our analysis of two-proton correlations we have used a Monte-Carlo program [4], which evaluates these wave functions and where detector acceptance and resolution was incorporated.

A simple theoretical picture of multi-pion production yields the following prediction for the two-particle correlation function [5]:

$$C_2 \equiv \frac{< n >^2}{< n(n-1) >} \cdot \frac{d^6N/dp_1^3dp_2^3}{d^3N/dp_1^3 \cdot d^3N/dp_2^3} = 1 + \lambda \cdot |\tilde{\rho}(p_1^\mu - p_2^\mu)|^2, \qquad (1)$$

where n is the pion multiplicity and d^3N/dp_i^3 and $d^6N/dp_1^3dp_2^3$ are the one-pion and two-pion inclusive yields. $\tilde{\rho}$ is the Fourier transform of the distribution of emitters; the most commonly chosen analytic expressions for $\tilde{\rho}$ contain a suitable correlation length R. While this parameter seems to measure dynamical properties of the produced strings in e^+e^- collisions [6, 7], it can provide geometrical information in medium energy heavy ion collisions ($E_{lab} \leq 2\,A\,\mathrm{GeV}$) [8, 9, 10, 11, 12].

The parameter λ, a correlation strength, was introduced for technical reasons [13]; it is expected to be $= 1$ for a completely chaotic source. Theoretically a value of $\lambda < 1$ can be ascribed to a certain amount of coherent production of pions [14], but in the experiment many different effects may reduce the measured value of λ.

The interpretation of pion interferometry measurements is however still not straightforward:

- The question of the relevant variables is not solved. There is in general no common rest frame for all particle pairs. In addition, the choice of the six fundamental degrees of freedom from the two four-momenta is not a priori defined. This is especially difficult, if one considers dynamic (expanding) sources.
- The meaning of the correlation strength parameter is unclear. It is however obvious [15] that one cannot ignore unexplained variations of its values.
- The extracted source sizes are *effective* values. The production through resonances, the evolution of the source and the mechanism of freeze-out are folded into these parameters.

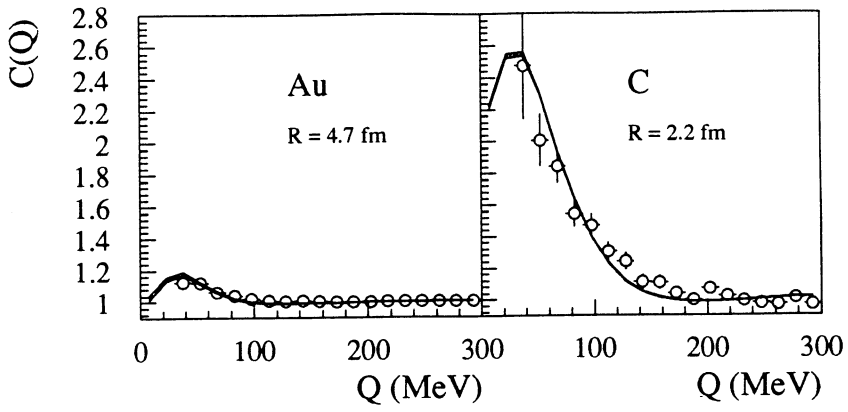

Fig. 1: Proton-proton correlation as a function of the invariant relative momentum Q for ^{16}O-induced reactions on Au and C targets at 200 AGeV. The circles show experimental data and the curves show the calculations. The width of the shaded area represents the statistical uncertainty of the numerical calculation.

But while absolute values extracted by interferometry analysis should be treated with caution, a comparison of different data sets may be most useful to learn both about the method itself and the dynamics of high energy collisions.

Experiments with ultrarelativistic nuclei have revealed the importance of rescattering of produced particles in the target spectator matter [16, 17]. Hints for pion absorption in the target nucleus are observed [18]. It is therefore of interest to study the target fragmentation region also by interferometric methods.

Data presented here have been taken in the WA80 experiment [19] at the CERN SPS with 200 AGeV proton, oxygen and sulfur beams. Protons and positive pions have been identified using the Plastic Ball detector [20]. A technical summary on the particle identification is given in table 1.

2 Proton correlations

Figure 1 shows experimental two-proton correlations as a function of $Q \equiv \sqrt{-(p_1^\mu - p_2^\mu)^2}$ together with fitted calculations for oxygen-induced reactions on Au and C targets. In the calculations Gaussian source distributions have been used. As expected, the most prominent feature is the increase of the resonance enhancement for smaller targets. This is well reproduced by the calculation, which establishes the fact, that the proton source is obviously smaller for smaller targets. Proton-induced reactions exhibit a similar behavior. To allow a more quantitative interpretation one can investigate the target mass dependence of the source radii. Figure 2 shows the radii extracted from pp correlations as a function of the cubic root of the target mass.

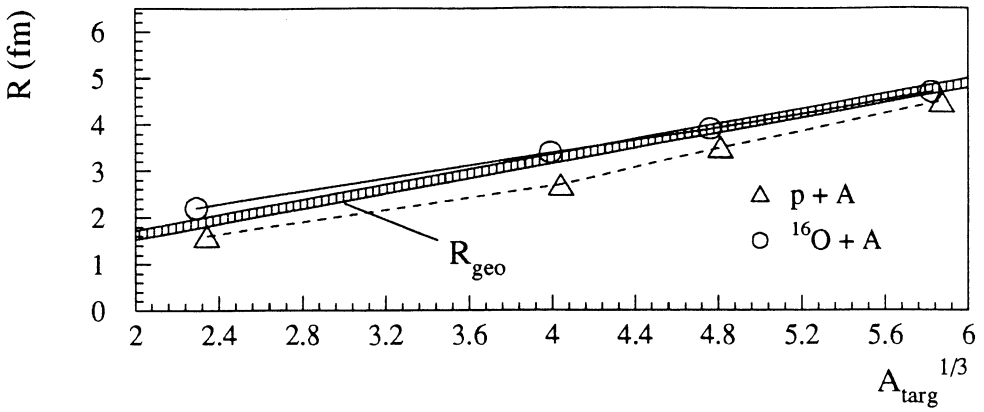

Fig. 2: Gaussian radius parameters extracted from two-proton correlations as a function of $A_{\rm target}^{1/3}$. The shaded band corresponds to Gaussian target radii parameterized as $A_{\rm target}^{1/3}$.

It can be clearly seen that the radii follow very closely a dependence of $A_{\rm target}^{1/3}$. The proton source seems to coincide with the target nucleus; the whole target nucleus is involved in rescattering processes.

The radii are slightly larger for oxygen-induced reactions than for proton-induced ones – both are however compatible with a geometric explanation.

3 Pion correlations

First results from pion interferometry analysis in the target region for ^{16}O-induced reactions have been published [21], where details of the analysis procedure are given. In the present paper the analysis is extended to other projectiles. In addition, a pair efficiency correction is introduced, which allows to measure pairs of smaller relative momentum than compared to [21]. This efficiency results from cross-talk via scattering of the decay-positrons into neighboring modules and has been determined from the data. Details of this efficiency correction will be given in a forthcoming publication.

The pion correlations discussed in this paper have been analyzed as a function of $Q_T \equiv |\vec{p}_{T1} - \vec{p}_{T2}|$ and $Q_L \equiv |p_{L1} - p_{L2}|$ simultaneously. Figure 3 shows as an example projections of the two-pion correlation function on Q_T and Q_L for 200 AGeV ^{32}S + Al. The data have been corrected for the Coulomb interaction with the standard Gamow factor [5] and with the additional efficiency correction.

Included in figure 3 are fits of a Gaussian parameterization:

$$C_2(Q_T, Q_L) = 1 + \lambda \cdot \exp\left(-\frac{Q_T^2 R_T^2}{2} - \frac{Q_L^2 R_L^2}{2}\right), \qquad (2)$$

which describes the data rather well.

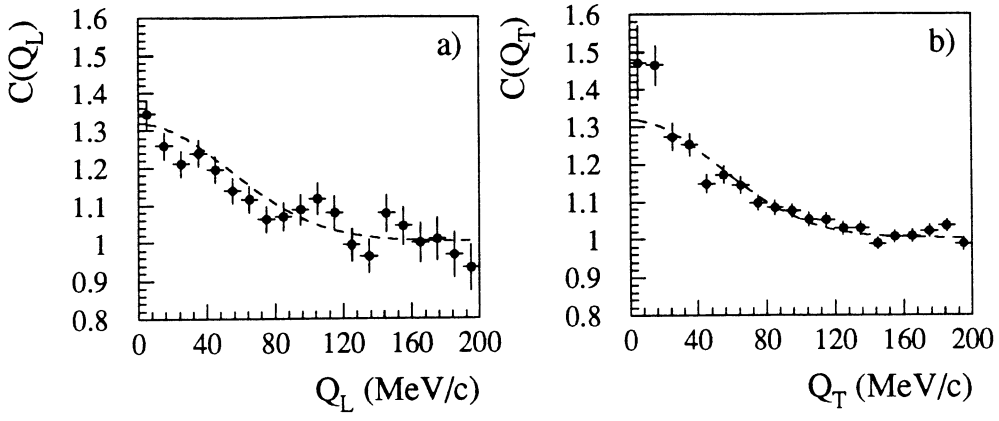

Fig. 3: Two-pion correlations as a function of Q_T and Q_L for 200 AGeV ^{32}S + Al a) projected onto Q_L for $Q_T \leq 50$ MeV/c a) projected onto Q_T for $Q_L \leq 50$ MeV/c. The dashed lines show Gaussian fits to the correlation function.

We have also looked at the target dependence of the extracted parameters. In figure 4 one can see R_T, R_L and λ as a function of $A_{target}^{1/3}$ for proton-, oxygen- and sulfur-induced reactions on various targets. Most astonishingly, the extracted radii do not follow the geometric expectation, but are more or less independently measured as $\approx$ 4fm for all systems. These values are much higher than expected for the light targets (esp. C).

People have expected an increase of transverse radii from expansion prior to freeze-out for phase-space regions of high particle density, i.e. at mid-rapidity. One would however not expect such a behavior for a system like p + C in the target region. At the same time, the radii for the Au target are *not* larger than the target nucleus, although the particle density is much higher in this case.

Another hint for the interpretation of these fits can be obtained from the values of λ. While λ is close to 1 for the C target, the values are much smaller for the heavier targets. As has been emphasized [15], one should not naively compare radii in such cases, because the parameters R and λ are not independent.

A closer look at correlation functions for the Au target, where high statistics are available, yields further information. Figure 5 shows projections of two-pion correlation functions on Q_T and Q_L in ^{32}S + Au reactions. For these projections very small bins in the orthogonal variable (10 MeV/c) have been used. One can clearly see that the Gaussian fits do not describe the data. The function completely misses the first data points. An exponential fit is slightly better (dotted line), but the best fit is provided by using a sum of two Gaussians as the source distribution - a second larger component is needed to account for the steep rise at small relative momentum. This easily explains, why the single Gaussian fits are meaningless at least for the Au target.

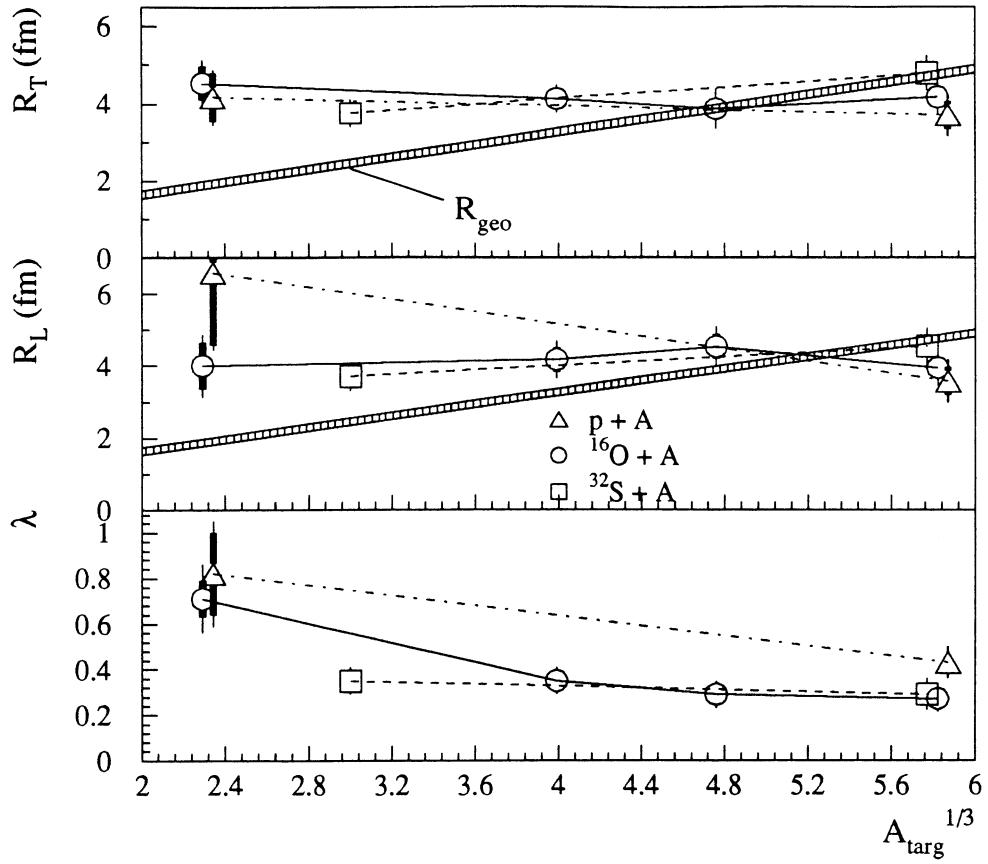

Fig. 4: Gaussian parameters R_T, R_L and λ extracted from two-pion correlations as a function of $A_{\text{target}}^{1/3}$. The shaded band corresponds to Gaussian target radii parameterized as $A_{\text{target}}^{1/3}$.

In figure 6 the systematic variation of the relative contributions $\lambda_{1,2}$ and the radii of the two components are displayed for reactions of p, ^{16}O and ^{32}S + Au. While the relative contributions are independent of the projectile mass, the radii increase with increasing A_{proj}. The radius of the smaller component is on the order of the projectile size, the second component however is much larger, reaching values of more than 15 fm. This two-component fit is however primarily a pragmatic approach. It has to be investigated, whether the shape is truly related to a two-component physical mechanism. In addition, a more realistic treatment of the Coulomb interaction may change the correlation function at very small relative momentum. This has to be studied, before one can draw conclusions on the production mechanism of the pions.

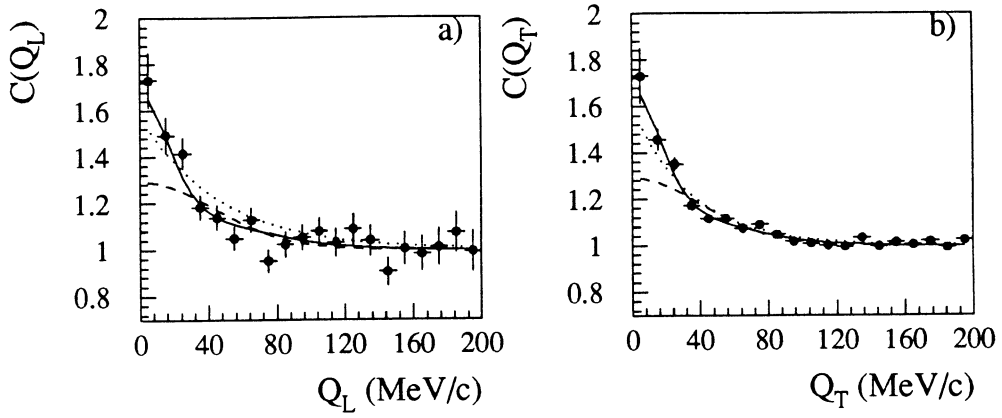

Fig. 5: Two-pion correlations as a function of Q_T and Q_L for 200 AGeV ^{32}S + Au a) projected onto Q_L for $Q_T \leq 10$ MeV/c a) projected onto Q_T for $Q_L \leq 10$ MeV/c. The dashed lines show Gaussian, the dotted lines exponential and the solid line double-Gaussian fits to the correlation function.

4 Summary

Correlations of soft pions and protons have been investigated in nucleus nucleus reactions in the target region. The extracted source parameters yield the following picture:

- The proton source seems to be identical to the target nucleus.
- The *effective* pion source is larger than the target nucleus for light targets.
- The correlation functions for the Au target cannot be described by single Gaussians. They indicate a very large second component of the pion source.

References

[1] R. Hanbury-Brown and R. Q. Twiss, Nature **178** (1956) 1046.

[2] G. Goldhaber et al., Phys. Rev. **120** (1960) 300–312.

[3] S. E. Koonin, Phys. Lett. **70 B** (1977) 43–47.

[4] S. Pratt, 1992, private communication.

[5] M. Gyulassy, S. K. Kauffmann, and L. W. Wilson, Phys. Rev. C **20** (1979) 2267–2292.

[6] M. G. Bowler, Z. Phys. C – Particles and Fields **29** (1985) 617–629.

[7] B. Andersson and W. Hofmann, Phys. Lett. **169 B** (1986) 364–368.

[8] D. Beavis et al., Phys. Rev. C **27** (1983) 910–913.

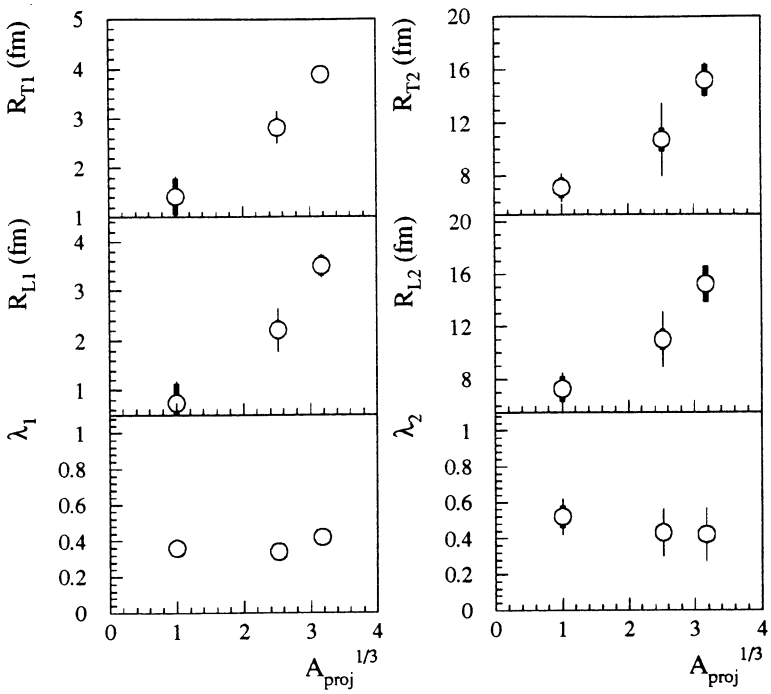

Fig. 6: Parameters of double-Gaussians extracted from two-pion correlations as a function of $A_{proj}^{1/3}$ for reactions on a Au target. The left hand side shows the smaller, the right hand side the larger component

[9] D. Beavis et al., Phys. Rev. C **28** (1983) 2561–2564.

[10] R. Bock et al., Z. Phys. A – Atomic Nuclei **333** (1989) 193.

[11] A. D. Chacon et al., Phys. Rev. Lett. **60** (1988) 780–783.

[12] W. A. Zajc et al., Phys. Rev. C **29** (1984) 2173–2187.

[13] M. Deutschmann et al., Nucl. Phys. **B 204** (1982) 333 – 345.

[14] R. M. Weiner, Phys. Lett. **B 232** (1989) 278.

[15] T. Peitzmann, Z. Phys. C – Particles and Fields **55** (1992) 485 – 489.

[16] R. Albrecht et al., Z. Phys. C – Particles and Fields **45** (1990) 529–537.

[17] R. Albrecht et al., Z. Phys. C – Particles and Fields **57** (1992) 37–42.

[18] H. Schmidt et al., Nucl. Phys. **A 544** (1992) 449c–454c.

[19] R. Albrecht et al., Study of Relativistic Nucleus-Nucleus Collisions at the CERN SPS, Aug. 1985, preprint CERN/SPSC/85-39 and GSI preprint 85-32.

[20] A. Baden et al., Nucl. Instr. and Meth. **203** (1982) 189.

[21] R. Albrecht et al., Z. Phys. C – Particles and Fields **53** (1992) 225–237.